IEEE Photonics Journal
An IEEE Photonics Society Publication

Open Access

Two-Photon-Excited Emission in Polymer Optical Fibers Doped With a Conjugated Polymer

Volume 6, Number 4, August 2014

I. Ayesta
M. A. Illarramendi
J. Arrue
F. Jiménez
J. Zubia

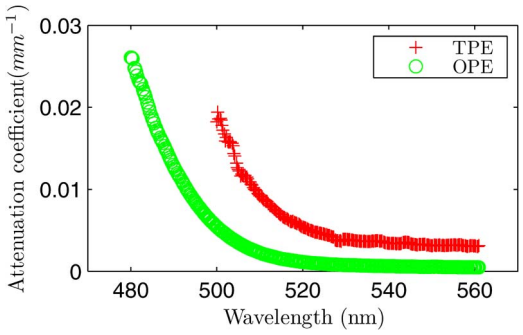

DOI: 10.1109/JPHOT.2014.2331238
1943-0655

IEEE photonics SOCIETY

IEEE

Two-Photon-Excited Emission in Polymer Optical Fibers Doped With a Conjugated Polymer

I. Ayesta,[1] M. A. Illarramendi,[2] J. Arrue,[1] F. Jiménez,[3] and J. Zubia[1]

[1]Department of Communications Engineering, University of the Basque Country UPV-EHU, 48013 Bilbao, Spain
[2]Department of Applied Physics I, University of the Basque Country UPV-EHU, 48013 Bilbao, Spain
[3]Department of Applied Mathematics, University of the Basque Country UPV-EHU, 48013 Bilbao, Spain

DOI: 10.1109/JPHOT.2014.2331238

Manuscript received April 15, 2014; revised June 2, 2014; accepted June 4, 2014. Date of publication June 26, 2014; date of current version July 14, 2014. This work was supported in part by the Ministerio de Economía y Competitividad under Project TEC2012-37983-C03-01; by the Gobierno Vasco/Eusko Jaurlaritza under Projects IT664-13, S-PE13CA004, and S-PE13UN151; and by the University of the Basque Country (UPV/EHU) through Program UFI11/16. Corresponding author: I. Ayesta (e-mail: igor.ayesta@ehu.es).

Abstract: In this paper, the two-photon-excited emission spectra of polymer optical fibers doped with the conjugated polymer Poly(9,9-dioctylfluorene-alt-benzothiadiazole) (F8BT) have been measured pumping the fibers transversely to their symmetry axis. Measurements include evolutions of the emission spectra with excitation wavelength and with propagation distance, together with an analysis of emission photostability. Comparisons with results for one-photon-excited emission are also presented and discussed.

Index Terms: Two-photon excitation, polymer optical fibers, organic materials, conjugated polymers, fluorescence.

1. Introduction

Two-photon-pumped fluorescence and lasing are very important because of their diverse applications in the fields of optical data storage, 3D micro- and nano-fabrication, optical limiting, biological imaging and photodynamic therapy. As compared to conventional one-photon lasing, two-photon-excited (TPE) lasing requires pumping at a much longer excitation wavelength, typically ranging from the red to the near-infrared spectral regions. These longer excitation wavelengths could be beneficial for the photostability of some materials. Besides, TPE lasing does not require phase matching, as would be necessary in frequency up-conversion based on second harmonic generation. TPE lasing has been demonstrated in many organic dyes in solvents [1] and also in several doped solid-state matrices [2], [3]. In the latter case, the use of optical fibers provides several advantages, such as optical confinement in a thin core, long interaction distance between the light and the gain medium, symmetric output of the beam profile, good adaptability to fiber-optic communications systems and high ratio between surface area and volume, which allows efficient heat dissipation and minimization of thermal degradation of performance. On the other hand, the use of optical fibers as host media facilitates sensing applications. For example, TPE fluorescence in rare-earth-doped optical fibers has been recently used for distributed sensing of temperature [4].

Although many studies of TPE fluorescence and of TPE lasing have been carried out in silica and glass optical fibers [5], [6], few works can be found in the literature about both phenomena in polymer optical fibers [7]–[9]. Poly (methyl methacrylate) (PMMA) polymer optical fibers (POFs) have raised a great interest in the last few years in applications such as short-haul communications links, sensing applications and, by using active dopants, also in the field of fiber lasers and amplifiers in the visible region [10]–[15]. It is also interesting to mention POFs made of the emerging polymer TOPAS, which present interesting properties, especially for sensing applications [12], [16]–[18]. POFs have the advantages of being robust, of having large core diameters and high numerical apertures, and of presenting lower manufacturing temperatures as compared to glass fibers. At such temperatures, the core of POFs can be manufactured with a wide variety of active materials embedded in it, such as organic dyes and conjugated polymers. Organic dyes with large absorption and emission cross sections can be easily embedded in the core of PMMA POFs to obtain high gains in particularly short fiber lengths [19]. It is also known that conjugated polymers can also yield high absorption coefficients and high fluorescence efficiency. Moreover, they are good candidates for optical switching due to their fast electronic transitions [20], [21]. These properties have led to a wide range of applications of these materials as optoelectronic devices [22].

In this work we analyze in detail the TPE emission features of PMMA POFs doped with the polyfluorene conjugated polymer Poly(9,9-dioctylfluorene-alt-benzothiadiazole) (F8BT). F8BT has been extensively used in organic light emitting diodes. It has also been employed in organic field-effect transistors and it is suitable even for organic solar cells. TPE fluorescence of conjugated polymers has been demonstrated in different structures, e.g. conjugated polymers in solvents, nanoparticles consisting of conjugated polymers, and films of a conjugated polymer blended with polystyrene [1], [23]–[25]. However, as far as we know, this is the first time that TPE emission in a POF doped with any conjugated polymer is reported. We study the dependence of the TPE emission spectra of F8BT-doped POFs on the excitation wavelength and on the light propagation distance, exciting the fibers transversely to their symmetry axis. The photostability of the TPE emitted fluorescence has also been analyzed. All the results obtained for TPE emission are compared with the corresponding results obtained for one-photon excited (OPE) emission.

2. Experimental Set-up

Measurements have been carried out using a PMMA step-index POF whose core is doped with F8BT with a concentration of 0.003 wt%. The cladding material is not doped. The fiber diameter is 1 mm, the core diameter being 980 μm and the cladding thickness being 10 μm. The doped fiber was produced by the POF manufacturer Luceat S.p.A (Italy) using an adapted preform-drawing technique and the manufacture details can be found in [20]. All fiber samples were 30–40 cm long and the fiber ends were carefully polished by hand using polishing papers.

Fig. 1 shows the set-up employed by us to measure the TPE fluorescence or emission spectra. The measured doped fiber was held between two *xy* micropositioners standing on a linear stage to maintain the working area of the fiber completely horizontal and to focus the incident laser beam properly. Active fibers were excited with a tunable femtosecond laser from 690 nm to 1040 nm (Mai Tai HP, laser pulses of $\sim$100 fs and a repetition rate of 80 MHz). The laser beam was focused onto the fiber side by means of a convergent lens of 7.5 cm of focal length. The impinging intensity could be controlled by adjusting manually the variable attenuator placed after the laser output. All the emission spectra obtained from the fiber end were measured by a USB4000 fiber-optic spectrometer with an optical resolution of 1.5 nm of full width at half maximum (FWHM), and the data obtained were corrected for the response of the detection system. In order to remove the pump power that could propagate through the fiber, a 10SWF-800-B short-pass filter with a cut-wavelength of 800 nm was inserted in a filter holder placed between the fiber end and the spectrometer. The holder (Avantes FH-Inline-1″) had two quartz collimating lenses and two SMA 905 connectors to facilitate light coupling into the spectrometer. A

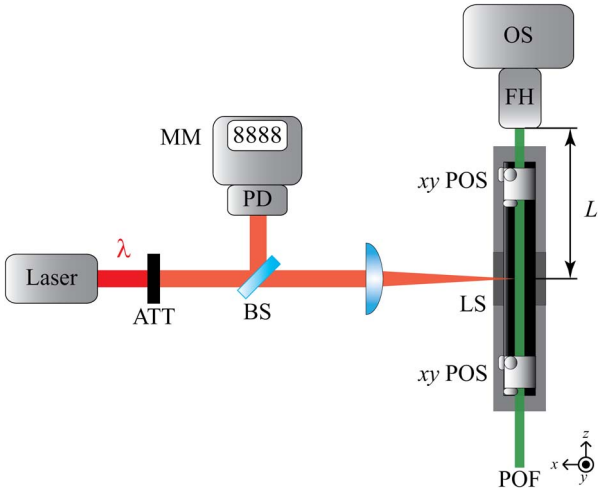

Fig. 1. Experimental set-up employed to measure the TPE emission spectra obtained from doped POFs. Legend: ATT: Variable Attenuator; BS: Beam Splitter; PD: Photodetector; MM: Multimeter; LS: Linear Stage; *xy* POS: *xy* micropositioner; FH: Filter Holder; OS: Optical Spectrometer.

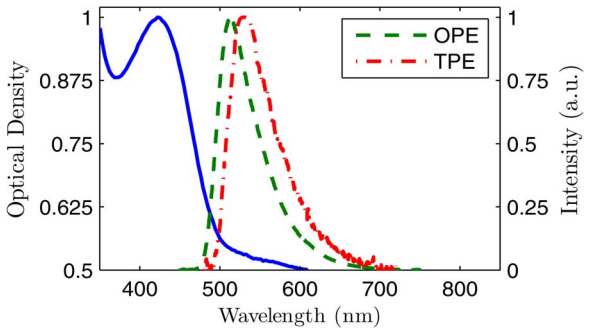

Fig. 2. OPE and TPE fluorescence spectra (dashed line and dash-dotted line) of the F8BT-doped POF with $L = 16$ cm. The excitation intensities are 0.97 Wcm^{-2} (at 400 nm) and 6250 Wcm^{-2} (at 800 nm). The solid line is the one-photon absorption spectrum.

reference signal was obtained using a beam splitter to cancel the intensity fluctuations of the laser. The variations of the TPE emission spectrum as light propagates along the doped fiber were obtained by changing the position of the launching point of the laser beam. An ILS250CC linear stage driven by an ESP300 motion controller was used for this purpose. Our own LabVIEW program was built to automate both the motion controller and the spectrometer. In the rest of the measurements, the distance L from the incidence point of the pump beam to the output end of the fiber closest to the spectrometer was constant (16 cm). Measurements of the OPE emission spectra were made in a previous work by employing a frequency-doubling unit (Inspire Blue) in a similar set-up but without focusing the beam onto the fiber [26]. Absorption spectra of the doped fiber were obtained from a Cary 50 UV-Vis spectrophotometer equipped with a fiber-optic coupler accessory. In these measurements, the fiber length was short enough (1 cm) to detect the absorption band of the dopant embedded in the fiber core.

3. Results and Discussion

The one-photon absorption spectrum and the TPE and OPE fluorescence spectra obtained for the F8BT-doped POF have been plotted in Fig. 2. It can be observed that the long-wavelength tail of the absorption band corresponding to the F8BT is overlapped with both emission spectra. This overlapping causes spectral changes in the output emission due to reabsorption and

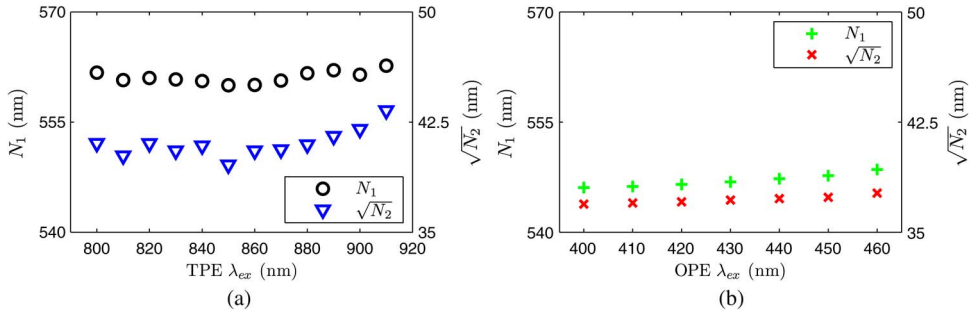

Fig. 3. Spectral characteristics of the emitted spectrum as a function of the excitation wavelength for both techniques. (a) TPE emission spectrum: N_1 (O) and $N_2^{1/2}$ (∇). (b) OPE emission spectrum: N_1 (+) and $N_2^{1/2}$ (x). The propagation distance is 16 cm in both cases. The excitation intensity is 6250 Wcm^{-2} in the two-photon excitation and 0.97 Wcm^{-2} in the one-photon one.

reemission effects that take place along the fiber [26], [27]. The excitation wavelength used for the TPE emission spectrum was $\lambda_{ex} = 800$ nm and the excitation intensity was high enough to detect emission from the fiber end, its value being 6250 Wcm^{-2}. The OPE emission was obtained exciting at 400 nm with an incident intensity of 0.97 Wcm^{-2}. Both emission spectra were measured with the same detection configuration and with the same light propagation distance along the fiber ($L = 16$ cm). In Fig. 2 we can see that the TPE emission spectrum is shifted towards longer wavelengths by 17 nm as compared to that obtained with one-photon excitation. Besides, it can be noticed that the TPE emission spectrum is slightly broader. Similar spectral behaviors have also been reported in other conjugated polymers and in other dopant materials in different structures, with various possible explanations, such as reabsorption effects [28] or inhomogeneous broadening in the polymer [29]. In our measurements with fiber, one of the reasons for this red shift could be the reabsorption effect. This effect is greater in the TPE emission measurements due to the point-excitation scheme employed. With a point excitation, the emitted rays travel longer distances along the fiber and, therefore, undergo greater red shifts than when a more extended region is excited and more parallel rays are emitted, as happens in the OPE emission set-up. Another reason could be the blue shift of emission that tends to occur as light travels along the stripe of fiber of a few millimeters excited by the laser in our one-photon set-up [30].

3.1. Excitation-Wavelength Dependence

The dependence of the TPE emission spectrum as a function of the excitation wavelength with a constant light propagation distance (16 cm) has been analyzed using the first and second moments of the spectra. The first moment N_1 represents the average emission wavelength and the square root of the second moment $N_2^{1/2}$ is proportional to the spectral width [26]. Fig. 3 shows the evolution of both parameters as the excitation wavelength changes. The values of N_1 and of $N_2^{1/2}$ of the OPE emission spectra have also been included for comparison. Note the absence of noticeable spectral changes in both excitation schemes, which means that the dopant molecule distribution in the PMMA matrix can be considered to be uniform [31]. In the analyzed wavelength range, the TPE emission spectra are red shifted in about 17 nm with respect to the OPE ones, and they are slightly broader as well, as was also shown before in Fig. 2.

3.2. Propagation-Distance Dependence

The evolution of the TPE emission spectra as a function of the light propagation distance z has been analyzed by exciting the fiber at 800 nm. When the excitation point is moved farther from the detector, the amount of measured emitted intensity is reduced, and the output emission spectrum is shifted towards longer wavelengths due to reabsorption and reemission effects. As

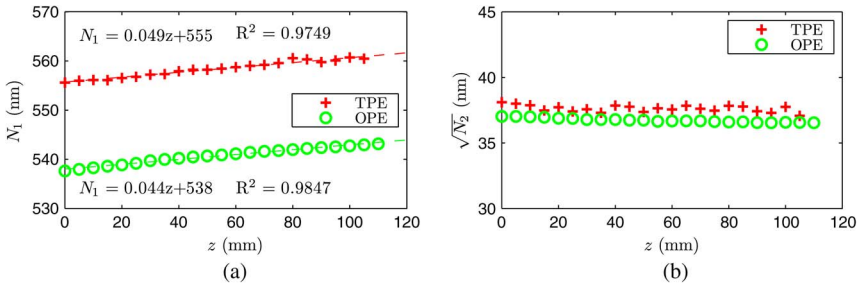

Fig. 4. Evolutions of both (a) N_1 and (b) $N_2^{1/2}$ of the TPE and OPE emission spectra as a function of the light propagation distance along the F8BT-doped POF. The incident intensity is 6250 Wcm^{-2} (at 800 nm) in the two-photon excitation (+) and 0.97 Wcm^{-2} (at 400 nm) in the one-photon excitation (O). The point of the fiber closest to the detector has been normalized to $z = 0$ The linear fittings in (a) are shown as dashed lines.

can be seen in Fig. 4(a), there is a fairly linear red shift of the first moment of the TPE emission spectra as the light propagation distance is increased. Regarding the spectral widths, Fig. 4(b) shows that there are not variations with the propagation distance. The evolution with z of the first moment of the OPE emission spectrum has also been plotted in Fig. 4(a). Although the TPE emission spectra are red shifted with respect the OPE spectra, both lines of N_1 have very similar slopes, namely 0.49 nm/cm and 0.44 nm/cm. This similarity seems to indicate that the overlap between the TPE and OPE emission spectra and the linear absorption spectrum should be approximately the same, but this fact is not reflected in Fig. 2. The effect of having a smaller overlap for the TPE emission spectrum (see Fig. 2) is probably compensated with the longer distance that the TPE emission travels along the fiber. This type of analysis can be useful to know the tunability for the emission of photonic devices based on doped POFs.

Due to the local excitation used in the TPE measurements, we can assume that the fluorescence is produced from one source placed just at the center of the fiber, i.e., from a point source. Therefore, the output intensity measured at an emission wavelength λ after propagating a distance z along the fiber can be expressed as follows [15]:

$$I(z,\lambda) = I_0(\lambda)\int_0^{\theta_c} \exp\left[-\frac{\alpha(\lambda)}{\cos\theta}z\right]\sin\theta\, d\theta \tag{1}$$

where $I_0(\lambda)$ is the intensity at the initial position, $\alpha(\lambda)$ is the linear attenuation coefficient at that wavelength, and θ_c the critical angle of propagation of the emission generated inside the POF with respect to its symmetry axis. For this doped fiber, the value for θ_c is approximately 20° for a point source [32]. We have worked out a new and simpler expression for (1) that is only valid when θ_c is small enough, as happens in our case, by truncating a series expansion of it around $\theta_c = 0$ The obtained expression is written as

$$I(z,\lambda) = I_0(\lambda)\exp[-\alpha(\lambda)z]\left(1 - \frac{\alpha(\lambda)z}{4}\theta_c^2 + \left(\frac{\alpha(\lambda)z}{48}(-3+2\alpha(\lambda)z)\right)\theta_c^4\right). \tag{2}$$

For the values of z used in this work and $\theta_c = 20°$, the intensities calculated from (1) and from (2) are practically identical. The maximum relative difference between them is 0.03% in the considered range of distances. Equation (2) fits properly to the experimentally measured intensities in the range of wavelengths of the tail of the absorption spectrum of the dopant, i.e., close to or inside the overlap between the absorption and TPE emission spectra. Out of this range, (2) does not fit properly due to reabsorption and reemission effects. In order to clarify this idea, in Fig. 5, we have plotted the transmitted TPE emission intensity as a function of the light propagation distance at two different wavelengths, one of them being located inside the overlap region (501 nm) and the other one outside it (578 nm). At $\lambda = 501$ nm, the transmitted intensity

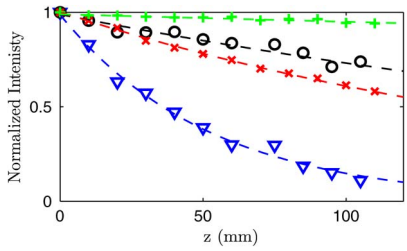

Fig. 5. Normalized transmitted intensity as a function of z at two different emission wavelengths: at 578 nm for both TPE emission (O) and OPE emission (+), and at 501 nm for both TPE emission (∇) and OPE emission (x). The intensity is 6250 Wcm^{-2} at 800 nm for the two-photon excitation and 0.97 Wcm^{-2} at 400 nm for the one-photon excitation. The dashed lines plotted for the TPE emission are the corresponding fittings using (2), with $R^2 = 0.99$ at 501 nm and $R^2 = 0.85$ at 578 nm. The other two dashed lines are the fittings for the OPE emission to exponential decays, with $R^2 = 0.99$ at 501 nm and $R^2 = 0.82$ at 578 nm.

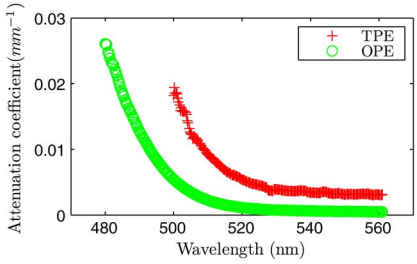

Fig. 6. Linear attenuation coefficients of the F8BT-doped POF for the TPE emission (+) and for the OPE emission (O).

fits well to (2), as can be seen in the coefficients of determination obtained. Out of the overlap region, the transmitted intensity does not follow the behavior predicted by (2) so well, because there is a reemission of the light absorbed at the tail of the short wavelengths of the emission band. The values of $\alpha(\lambda)$ obtained from the fittings to (2) in the appropriate spectral range have been plotted in Fig. 6. Figs. 5 and 6 also include the corresponding measurements analyzed for one-photon excitation, in which an approximately plane-wave source has been considered due to the extended excitation [26]. In this case, the values of $\alpha(\lambda)$ have been calculated from the fittings of the output intensities to the typical Beer–Lambert exponential decay. Notice that the values of $\alpha(\lambda)$ are larger for the TPE emission than for the OPE one. This difference cannot be explained from the different geometries of the emission source, since the calculated variations in $\alpha(\lambda)$ if the type of light source is changed are too small (less than 10%). However, the lower attenuation of light propagating in the cladding could be a possible explanation of the differences in $\alpha(\lambda)$ obtained with both techniques. Specifically, there is possibly smaller coupling of the TPE emission into the cladding, where the attenuation is much smaller.

3.3. Photostability

The photostability of the TPE emission spectra has been analyzed pumping the F8BT-doped fibers in two tests. In the first one, we pumped the fibers for 60 minutes at 800 nm with 6250 Wcm^{-2} [see Fig. 7(a)]. After a rest interval in which the samples were in darkness and at room temperature for 24 hours, the fibers were exposed again in a second test for another 60 minutes under the same conditions [see Fig. 7(b)]. In the first test, the doped fibers had never been exposed to laser light, so there was no previous degradation that could affect the results, and in the second one light was launched at exactly the same point of the fiber. Photostability measurements carried out pumping the fibers with one-photon excitation have also been included in Fig. 7(a) and (b). For the sake of comparison, we have normalized both

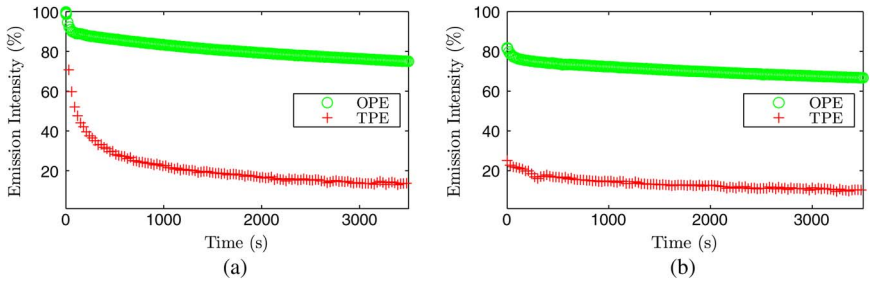

Fig. 7. TPE (+) and OPE (O) emission intensity as a function of the excitation time. The excitation intensity is 6250 Wcm^{-2} (at 800 nm) and 0.97 Wcm^{-2} (at 400 nm), respectively, and the light propagation distance is 16 cm. (a) Fibers excited for up to 60 minutes. (b) Excitation for another 60 min. after a day at rest.

TABLE 1

Values of the fittings to the experimental curves of Fig. 7(a) with (3)

	τ_1 (s)	τ_2 (s)	R^2
Two photon	101,50	3568	0,98
One photon	48,73	20934	0,99

emission intensities to 100% at the start of the first test. As could be expected, due to the higher intensity employed, the photostability of the TPE emission is inferior to that of the OPE one. Specifically, after 60 minutes of exposure at 80 MHz (equivalent to $2.88 \cdot 10^{11}$ laser shots), the TPE emission capacity is reduced by 76%, whereas the reduction for the case of one-photon excitation is only of 25% after the same period. After 24 hours of rest in darkness, there is a partial recovery in the emission capacity in both cases. Fig. 7(b) shows that the emissions are initially 12% and 7% higher than at the last point of the first excitation period for two-photon and for one-photon excitation techniques, respectively. The decays in the first test can be fitted by a double exponential function of the form [26]

$$f(t) = a\,\exp(-t/\tau_1) + b\,\exp(-t/\tau_2) \tag{3}$$

in which a and b are constants and τ_1 and τ_2 represent the decay times in the short term and in the long term, respectively. The calculated values of these decay times are shown in Table 1, together with the coefficients of determination. Notice that larger values of τ_2 suggest that the slope with time in the long term is smaller, i.e., that the photostability is better. The values of τ_2 shown in Table 1 for both excitation conditions corroborate that the sample excited by the one-photon technique is more stable in the long term.

None of the excitation schemes yields significant spectral changes of the generated emission with excitation time. This spectral stability could be related to a homogeneous distribution of the dopant in the matrix [33]. The photodegradation in doped PMMA polymers is a phenomenon that limits the applicability of such materials, which is not well understood yet. Efforts are being done to solve this problem, such as the application of an adequate electric field to control the decay and the recovery processes and to increase the threshold damage [34].

4. Conclusion

For the first time, two-photon-excited emission from a conjugated polymer (F8BT) embedded in a polymer optical fiber has been measured pumping the fiber transversely to its symmetry axis. It has been demonstrated that the two-photon-excited emission spectra can be tuned by changing the fiber length. From the analysis of the two-photon-excited emission with propagation distance along the fiber, we have characterized the optical losses in the doped fiber. The results of the two-photon and one-photon excited emissions have been compared. It has been found that

the two-photon-excited emission spectra are red shifted and slightly broader. It has also been shown that the emission intensity generated by two-photon excitation is more attenuated along the fiber and that its photostability is lower. These effects can be related to the local excitation of high intensity employed in the two-photon excitation, as well as the specific geometry of polymer optical fibers, in the sense that they consist of a doped core and an undoped cladding. We expect that this work will promote further advances in the field of non-linear optical properties of polymer optical fibers for diverse applications, such us the implementation of alternative pumping schemes for compact lasers and amplifiers based on polymer optical fibers, or the achievement of compact fiber sensors for industry and biomedicine.

References

[1] G. S. He, L. Tan, Q. Zheng, and P. N. Prasad, "Multiphoton absorbing materials: Molecular designs, characterizations, and applications," *Chem. Rev.*, vol. 108, no. 4, pp. 1245–1330, Apr. 2008.

[2] X. H. Yang, J. M. Hays, W. Shan, J. J. Song, and E. Cantwell, "Two-photon pumped blue lasing in bulk ZnSe and ZnSSe," *Appl. Phys. Lett.*, vol. 62, no. 10, pp. 1071–1073, Mar. 1993.

[3] G. S. He, C. F. Zhao, J. D. Bhawalkar, and P. N. Prasad, "Two-photon pumped cavity lasing in novel dye doped bulk matrix rods," *Appl. Phys. Lett.*, vol. 67, no. 25, pp. 3703–3705, Dec. 1995.

[4] C. J. Dalzell, T. P. J. Hanl, S. Ruddock, and D. B. Hollis, "Two-photon excited fluorescence in rare-earth doped optical fiber for applications in distributed sensing of temperature," *IEEE Sensors J.*, vol. 12, no 1, pp. 51–54, Jan. 2012.

[5] M. J. F. Digonnet, Ed., *Rare-Earth-Doped Fiber Lasers and Amplifiers, Revised and Expanded*, 2nd ed. New York, NY, USA: Marcel Dekker, 2001.

[6] X. Zhu and N. Peyghambarian, "High-power ZBLAN glass fiber lasers: Review and prospect," *Adv. OptoElectron.*, vol. 2010, pp. 501956-1–501956-23, Jan. 2010.

[7] G. Jordan, T. Kobayashi, W. J. Blau, S. Pfeiffer, and H. Hörhold, "Frequency upconversion of 800 nm ultrashort pulses by two-photon absorption in a stilbenoid compound-doped polymer optical fiber," *Adv. Funct. Mater.*, vol. 13, no. 10, pp. 751–754, Oct. 2003.

[8] M. Sheeba *et al.*, "Side illumination fluorescence emission characteristics from a dye doped polymer optical fiber under two-photon excitation," *Appl. Opt.*, vol. 47, no. 11, pp. 1913–1921, Apr. 2008.

[9] G. S. He, J. D. Bhawalkar, C. F. Zhao, C. K. Park, and P. N. Prasad, "Upconversion dye-doped polymer fiber laser," *Appl. Phys. Lett.*, vol. 68, no. 25, pp. 3549–3551, Jun. 1996.

[10] J. Zubia and J. Arrue, "Plastic optical fibers: An introduction to their technological processes and applications," *Opt. Fiber Technol.* vol. 7, no. 2, pp. 101–140, Apr. 2001.

[11] H. Z. Yang *et al.*, "A review of recent developed and applications of plastic fiber optic displacement sensors," *Measurement*, vol. 48, pp. 333–345, Feb. 2014.

[12] A. Argyros, "Microstructures in polymer fibres for optical fibres, THz waveguides, and fibre-based metamaterials," *ISRN Opt.*, vol. 2013, pp. 785162-1–785162-22, 2013.

[13] *Proc. Int. Conf. POF*, conference edited by Prof. M. M. Werneck. [Online]. Available: http://www.pof2013.org.br/pof2013/index.php?option=com_content&view=article&id=58&Itemid=66

[14] D. Amarasinghe, A. Ruseckas, G. A. Turnbull, and I. D. W. Samuel, "Organic semiconductor optical amplifiers," *Proc. IEEE*, vol. 97, no. 9, pp. 1637–1650, Sep. 2009.

[15] M. G. Kuzyk, *Polymer Fiber Optics: Materials, Physics, and Applications*. Boca Raton, FL, USA: CRC, 2007.

[16] W. Yuan *et al.*, "Humidity insensitive TOPAS polymer fiber Bragg grating sensor," *Opt. Exp.*, vol. 19, pp. 19 731–19 739, Sep. 2011.

[17] I.P. Johnson *et al.*, "Optical fibre Bragg grating recorded in TOPAS cyclic olefin copolymer," *Electron. Lett.*, vol. 47, no. 4, pp. 271–272, Feb. 2011.

[18] G. Emiliyanov, P. E. Hoiby, L. H. Pedersen, and O. Bang, "Selective serial multi-antibody biosensing with TOPAS microstructured polymer optical fibers," *Sensors*, vol. 13, pp. 3242–3251, Mar. 2013.

[19] A. Tagaya, S. Teramoto, E. Nihei, K. Sasaki, and Y. Koike, "High-power and high-gain organic dye-doped polymer optical fiber amplifiers: Novel techniques for preparation and spectral investigation," *Appl. Opt.*, vol. 36, no. 3, pp. 572–578, Jan. 1997.

[20] A. Charas *et al.*, "Gain and ultrafast optical switching in PMMA optical fibers and films doped with luminescent conjugated polymers and oligomers," *Front. Optoelectron. China*, vol. 3, no. 1, pp. 45–53, Mar. 2010.

[21] J. Clark *et al.*, "Blue polymer optical fiber amplifiers based on conjugated fluorene oligomers,"*J. Nanophoton.*, vol. 2, no. 1, pp. 023504, Mar. 2008.

[22] J. Clark and G. Lanzani, "Organic photonics for communications," *Nat. Photon.*, vol. 4, no. 7, pp. 438–446, Jul. 2010.

[23] C. Wu, C. Szymanski, Z. Cain, and J. McNeill, "Conjugated polymer dots for multiphoton fluorescence imaging," *J. Amer. Chem. Soc.*, vol. 129, no. 43, pp. 12 904–12 905, Oct. 2007.

[24] H. Wang, Z. Li, P. Shao, J. Qin, and Z. Huang, "Two-photon absorption property of a conjugated polymer: Influence of solvent and concentration on its property," *J. Phys. Chem. B*, vol. 114, no 1, pp. 22–27, Jan. 2010.

[25] G. Sreelekha *et al.*, "Two photon fluorescence spectra from MEH-PPV/polystyrene based film waveguides," *J. Opt.*, vol. 42, no. 2, pp. 101–105, Jun. 2013.

[26] I. Ayesta *et al.*, "Luminescence study of polymer optical fibers doped with conjugated polymers," *J. Lightw. Technol.*, vol. 30, no. 21, pp. 3367–3375, Nov. 2012.

[27] M. A. Illarramendi *et al.*, "Spectroscopic characterization of plastic optical fibers doped with fluorene oligomers," *J. Lightw. Technol.*, vol. 27, no. 15, pp. 3220–3226, Aug. 2009.
[28] J. Yu *et al.*, "Confinement of pyridinium hemicyanine dye within an anionic metal–organic framework for two-photon-pumped lasing," *Nat. Commun.*, vol. 4, Oct. 2013.
[29] A. Narayanan, O. P. Varnavski, T. M. Swager, and T. Goodson, "Multiphoton fluorescence quenching of conjugated polymers for TNT detection," *J. Phys. Chem. C*, vol. 112, no. 4, pp. 881–884, Jan. 2008.
[30] J. Arrue, F. Jimenez, I. Ayesta, M. A Illarramendi, and J. Zubia, "Polymer-optical-fiber lasers and amplifiers doped with organic dyes," *Polymers*, vol. 3, no. 3, pp. 1162–1180, Jul. 2011.
[31] M. N. Berberan-Santos, *Fluorescence of Supermolecules, Polymers, and Nanosystems*, vol. 4. New York, NY, USA: Springer-Verlag, 2008, ser. Springer Series on Fluorescence.
[32] I. Bikandi, M. A. Illarramendi, J. Zubia, J. Arrue, and F. Jiménez, "Side-illumination fluorescence critical angle: Theory and application to F8BT-doped polymer optical fibers," *Opt. Exp.*, vol. 20, no. 4, pp. 4630–4644, Feb. 2012.
[33] G.-D. Peng, Z. Xiong, and P. L. Chu, "Fluorescence decay and recovery in organic dye-doped polymer optical fibers," *J. Lightw. Technol.*, vol. 16, no. 12, pp. 2365–2372, Dec. 1998.
[34] B. Anderson, S. Hung, and M. G. Kuzyk, "Influence of an electric field on photodegradation and self-healing in disperse orange 11 dye-doped PMMA thin films," *J. Opt. Soc. Amer. B, Opt. Phys.*, vol. 30, no. 12, pp. 3193–3201, Dec. 2013.